
Chapter 5

Characterization of PAM/PEO Blends

Abstract

This chapter gives an account of the characteristics of PAM/PEO blend in different weight proportion (70/30, 50/50 and 30/70) which is prepared by solution cast technique. These blends are investigated by spectroscopic techniques like FTIR, UV-Vis and RAMAN. Mechanical, Thermal and Morphological properties are also investigated. The results obtained from different characterization techniques show the blending effect on different properties. These properties of PAM/PEO blends are correlated with spectroscopic investigation.

5.1. Introduction

Blending of polymers is an interesting as well as important route for providing new materials with desirable properties with economically low cost [1]. The properties of polymer blend can be controlled by blend morphology, blend composition and its processing condition [2]. The study of blend properties are very important to find its new applications in the field of biomedical and pharmacy [3, 4]. Polymer compatibility is an important criterion when dealing with blends. Polymer-polymer miscibility arises due to any specific interaction such as hydrogen bonding, dipole-dipole interaction or charge transfer process for pure polymer mixtures [5-8].

Due to increase in the applications of polymer in biomedical field, study of water soluble polymer like Poly (ethylene oxide) (PEO), poly (vinyl alcohol) (PVA), and polyacrylamide (PAM) have great interest [9, 10]. It is important to note that there are only very few studies on their blends. Polyacrylamide is used in multitude applications including water clarification, waste water treatment, oil recovery, agriculture and biomedical applications [11-13]. The high bio-adhesive property of acrylic polymers offers good prospects for using these polymers in controlled drug delivery systems for local applications [14, 15]. Structural and physical properties of elements doped PAM are far studied [16].

PEO is semi crystalline synthetic polymer. Because of its biocompatibility; it is used in many biomedical devices including drug delivery and tissue replacement [17-19]. PEO/Starch blends present great application in scaffolds for cell culture and tissue engineering [20, 21]. PEO has moderate tensile strength and it possesses good mechanical and electrical properties [22]. Some work is reported on optical and electrical properties of PEO based polymer electrolyte film [23-25]. Ferreiro et. al. reported that, when there is a change in blend ratio of PEO/PMMA, morphological transitions occurs [26, 27]. Chemical structure of PEO (presence of ether oxygen

and -OH end groups) makes some possibilities of hydrogen bonds formation, as it was already confirmed for e.g. PEO/poly (vinyl alcohol) and PEO/unsaturated polyester resin systems shows hydrogen bonding interaction [28, 29].

PAM and PEO individually blend with other polymers but to the best of our knowledge, there is no study of interaction of PAM and PEO polymer blends together. Only Vijayalakshmi et. al. has been studied thermal degradation characterization of blend of PEO and PAM [30, 31]. So the authors spot light on the preparation of solid films of PAM and PEO blends and also on the structural, thermal, optical, mechanical properties and morphological study of these blends. By means of FTIR and Raman spectroscopy, authors gives information regarding the intermolecular interaction between two polymer chains of PAM and PEO, which is quite helpful for the study of compatibility and miscibility of blends and the results were correlated with the results obtained from the other characterization techniques.

5.2. Results and Discussion

5.2.1. FTIR Analysis

FTIR spectroscopy of blend films were carried out to detect peak shifts, which may be due to interaction like hydrogen bonding between two polymers. Infrared spectroscopy is a fundamental technique to find out the presence of hydrogen bond which is characterized by changes in absorption bands of functional groups, which involved in the formation of hydrogen bond [32]. As absorption of the functional groups changes, it changes the force constant of donor and acceptor groups and due to this, frequencies of stretching and deformation of these groups are changing [32].

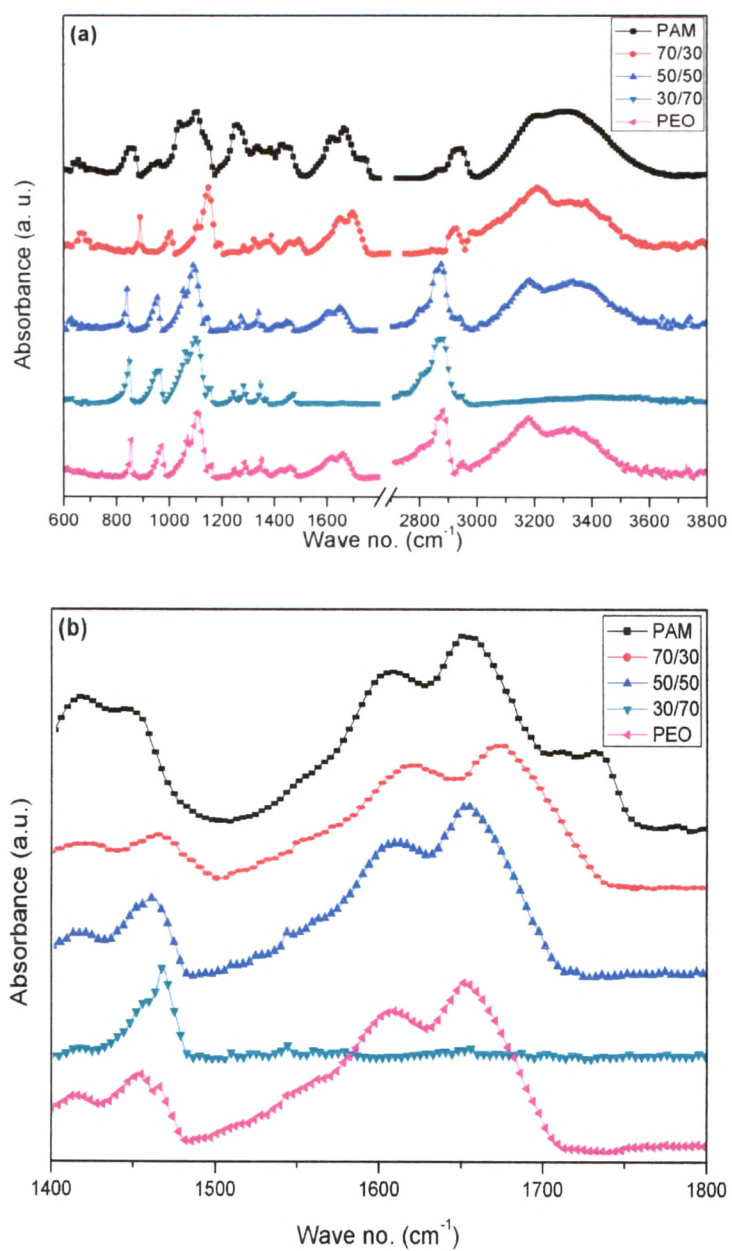


Figure 5.1 FTIR Spectra of Pure and blend polymers (a) in the region of 600-3800 cm⁻¹ (b) in the region of 1400-1800 cm⁻¹

Figure 5.1 shows the spectra of pure polymers and blend films. Peak values for pure and blend polymers are shown in Table 5.1. PAM has two bands at 3315 cm^{-1} and 3212 cm^{-1} indicates N-H stretching vibrations and absorption peak at 1651 cm^{-1} is due to C = O stretching, a peak at 1607 cm^{-1} is attributed to N-H bending and at 1447 cm^{-1} is due to C-N stretching vibrations [33, 34]. Poly Ethylene Oxide has two strong absorption bands at 3332 cm^{-1} and 3177 cm^{-1} which indicates -OH stretching vibrations and absorption band at 2881 cm^{-1} is for asymmetric stretching of $-\text{CH}_2$ group. Peaks at 1610 cm^{-1} and 1655 cm^{-1} indicate bound H_2O solvent in PEO polymer matrix in crystal form [34].

Compared with the pure polymers, for PAM/PEO blends, the absorption bands at $3000\text{-}3600\text{ cm}^{-1}$ corresponding to -OH and -NH stretching vibrations, the intensity of peaks decreases and clearly shifted peaks indicates the formation of strong intermolecular hydrogen bonding between the $-\text{CONH}_2$ group of Polyacrylamide and -OH group of Poly Ethylene Oxide. For 70/30 wt% of PAM/PEO blend, this shift is maximum on higher wave number side, so it has strong tendency for the formation of strong hydrogen bond [32, 35]. As we increase content of PEO in the blend, the above peak intensity starts decreasing and becomes very weak for 30/70 wt%. In the region $1400 - 1800\text{ cm}^{-1}$ we observed four important peaks. The C-N stretching vibration of PAM shifted to higher wave number (1447 to 1469 cm^{-1}) and the $-\text{CH}_2$ scissoring vibration of $-\text{CH}_2\text{OH}$ group of PEO also tends to shift towards higher wave number (1454 to 1469 cm^{-1}). The N-H bending vibration of PAM is observed at 1607 cm^{-1} . For blends it also shifts towards higher wave number (1607 to 1620 cm^{-1}). Peak at 1651 cm^{-1} , due to C=O stretching vibration of $-\text{CONH}_2$ group of PAM is also shifted to higher wave number side to 1678 cm^{-1} . These peak shifting observations support the formation of hydrogen bonding between $-\text{CONH}_2$ group of

Table 5.1 Assignments of the FT-IR characterization of bands of the pure PAM, pure PEO and PAM/PEO blend [16, 18, 36-38].

Wave no. (cm ⁻¹)	Peak Assignment (PAM)	Wave no. (cm ⁻¹)	Peak Assignment (PEO)	70/30 (wt %)	50/50 (wt %)	30/70 (wt %)
857	C-C Symmetric stretching	852	C-C Symmetric stretching	855	858	852
956	C-C Asymmetric stretching	966	-CH ₂ rocking	974	974	956
1107	C-O-C stretching	1106	C-O-C stretching	1119	1107	1095
1447	C-N stretching	1454	-CH ₂ scissoring	1469	1457	1469
1607	N-H bending	1610	Bound H ₂ O in PEO	1620	1609	weak
1651	C=O Stretching	1655	matrix as solvent	1678	1654	weak
2938	C-H Asymmetric stretching	2881	C-H Asymmetric stretching	2950	2893	2875
3212	N-H Symmetric stretching	3177	-OH stretching	3229	3195	weak
3315	N-H Asymmetric stretching	3332	-OH stretching	3371	3354	weak

PAM and -CH₂OH group of PEO. In this region maximum peak shift is observed for 70/30 wt% on higher wave number side. From all the blend spectra, peaks shift are observed for all blends, indicating that the intermolecular interaction occurs between two polymer chains. But for 70/30 wt% of PAM/PEO blend, maximum peak shift on higher wave number side are observed due to maximum intermolecular interaction. This indicates that the bond strength for 70/30 wt% is increased.

Final conclusion from all FTIR spectra can be drawn is that intermolecular interactions of hydrogen bonding with increasing bond strength between -CONH₂ group of PAM and -CH₂OH group of PEO were confirmed by FTIR spectra and it is maximum for 70/30 wt%. Due to which we are getting higher mechanical and thermal properties of blend films.

5.2.2. UV-Vis Analysis

The absorption of light energy by polymeric materials in the UV-Vis region involves transition of electrons in σ , π and n-orbital from the ground state to higher energy states. [43-45]. The optical absorption method can be used for the investigation of the optically induced transitions and can provide information about the band structure and energy gap in crystalline and non-crystalline materials [46].

The absorbance process plays an important role in the optical properties of the polymers. The absorption coefficient was determined from the UV-VIS spectra using the formula:

$$\alpha = A/d \quad (1)$$

Where A is the absorbance and d is the thickness of the film. The Tauc relation for dependence of absorbance on photon energy is [47]:

$$\alpha(\nu) = B(h\nu - E_g)^x/h\nu \quad (2)$$

Where $\alpha(\nu)$ is the absorption coefficient, E_g is the optical energy gap of the substance, h is plank's constant, ν is the corresponding frequency, x is the parameter that gives the type of electron transition. It was observed that two distinct linear relations were found for $x = 1/2$ (Direct transition) and $x = 2$ (Indirect transition), corresponding to different inter band absorption processes and factor B depends on the transition probability and can be assumed to be constant within the optical frequency range [48, 49] E_g is the optical energy gap. On the basis of equation 2, direct and indirect band gap and absorption edge were determined.

Absorbance and band edges

Figure 5.2 (a) shows the absorption spectra of the Pure and blended polymer films. From the spectra, peak height increases, band edge increases and the absorption band is found to shift towards shorter wavelengths with increasing the weight percentage of PEO. The optical absorption coefficient (α) was determined from the absorption spectra using equation (1). The plot of absorption coefficients (α) versus photon energy ($h\nu$) of the pure and blended polymer films are shown in Figure 5.2 (b). The position of the absorption edge values were calculated by extrapolating the linear portions of this plots to zero absorption values as shown in Table 5.2.

Direct and indirect optical band gap

The optical band gap of the Pure and blend samples was determined from the UV–Vis spectra. The value of the optical direct and indirect energy gap is determined from the intersection of the extrapolated line of the curves with the photon energy axis at zero absorption value. In an allowed direct transition the electron is simply transferred vertically from the top of the valence band to the bottom of the conduction band, without a change in momentum (wave vector) [50]. For the determination of the direct optical band gap, $(\alpha h\nu)^2$ was plotted as a function of photon energy ($h\nu$) as shown in Figure 5.2 (c).

In indirect band gap, a transition from the valence to the conduction band should always be associated with a phonon of the right magnitude of crystal momentum [48]. For indirect transition photon assistance requires. Indirect band gaps are obtained from the plots of $(\alpha h\nu)^{1/2}$ versus photon energy ($h\nu$) as shown in Figure 5.2 (d). The values of direct and indirect band gap for the pure and blended films are listed in Table 5.2. From the Table 5.2, it is seen that direct and indirect band gap increases with increasing PEO percentage.

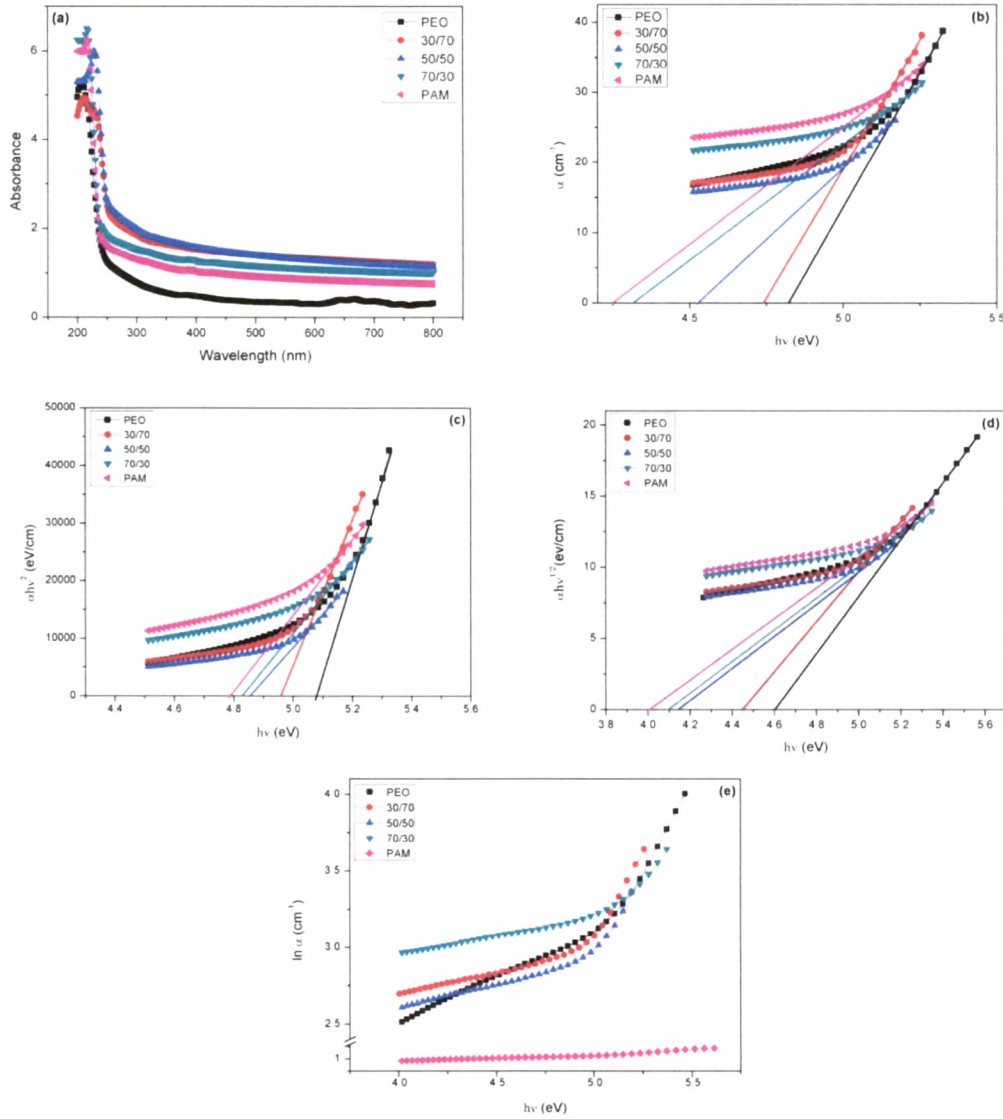


Figure 5.2 Plot of (a) Absorption coefficient (α) vs Wavelength (λ), (b) Absorption coefficient (α) vs Photon Energy ($h\nu$), (c) $(\alpha h\nu)^2$ vs $h\nu$, (d) $(\alpha h\nu)^{1/2}$ vs $h\nu$, (e) $\ln \alpha$ vs Photon Energy ($h\nu$)

This increase in the optical band gap values is due to the formation of defects due to the blending, and the interaction between the polymer chains [51-53] and the formation of some bonds [54]. As the crystalline nature of the films increases, the charge carrier cannot find a continuous chain to travel which causes the increase in the band gap, which in turn shows the effect of blending on the optical properties [48].

Activation energy

The optical activation energy can be determined using the Urbach rule [55] as

$$\alpha = B \exp(h\nu/E_a) \quad (3)$$

Where B is a constant and E_a is the activation energy, i.e. the inverse slopes of the exponential edge. The latter is interpreted as the width of the tail of localized states extending into the forbidden band gap from either the valence or conduction band [49].

The values of activation energy E_a is determined by taking the reciprocals of the slopes of the linear portions of plots of $\ln \alpha$ versus photon energy ($h\nu$) as shown in Figure 5.2 (e). The values of E_a for the Pure and blended doped films are listed in Table 5.2 and it increases with PEO wt%.

Table 5.2 Absorption edge, optical band gap (both direct and indirect) and activation energy values of pure PAM, pure PEO and PAM/PEO polymer blend films.

Composition (PAM/PEO)	Absorption edge (eV)	Direct Band gap (eV)	Indirect Band gap (eV)	Activation energy E_a (eV)
100/0	4.26	4.79	4.01	0.59
70/30	4.34	4.83	4.09	0.88
50/50	4.55	4.86	4.15	1.96
30/70	4.74	4.96	4.45	2.11
0/100	4.83	5.07	4.59	2.38

5.2.3. RAMAN Analysis

The Raman spectroscopy is a suitable and efficient method for the structural analysis of polymers. It is possible to characterize molecular bonds in various phase and conformational states with the help of Raman spectroscopy. If two polymers are fully or partially miscible then, their Raman spectra have considerable difference in band position and shapes between the spectra of blend and each of the pure polymers [39].

Distinctive differences between PAM and PEO can be observed from their Raman spectra as shown in Figure 5.3 (a, b). Raman peak values for pure and blend polymers are shown in Table 5.3. The bands near 854 cm^{-1} corresponding to C-C stretching region of PAM. The bands at 1107 cm^{-1} are attributed to the C-O-C stretching modes of PAM. The band near 1400 cm^{-1} is assigned mainly to the C-N stretching vibration and a band near 1711 cm^{-1} is attributed to C=O stretching mode of the PAM polymer chain.

For PEO, it is possible to observe the intense bands at 847 cm^{-1} and 1104 cm^{-1} , corresponding to the stretching modes of C-C and C-O respectively. The Raman band at 1336 cm^{-1} , 1454 cm^{-1} and 1633 cm^{-1} is correspondingly assigned to the $-\text{CH}_2$ wagging, $-\text{CH}_2$ deformation and $-\text{CH}_2$ twisting.

Peak shift is observed for all blends, which indicates the intermolecular interaction between two polymer chains. Maximum peak shift are observed for 70/30 wt% of PAM/PEO blend due to maximum intermolecular interaction. In the range of the stretching vibrations of the $-\text{CH}_2$ and $-\text{CH}_3$ groups, an increase in the PEO content causes an increase in the intensity of the line assigned to the symmetrical vibration of the $-\text{CH}_2$ group and a simultaneous monotonic shift of the peak position of this line from 2919 cm^{-1} to 2879 cm^{-1} .

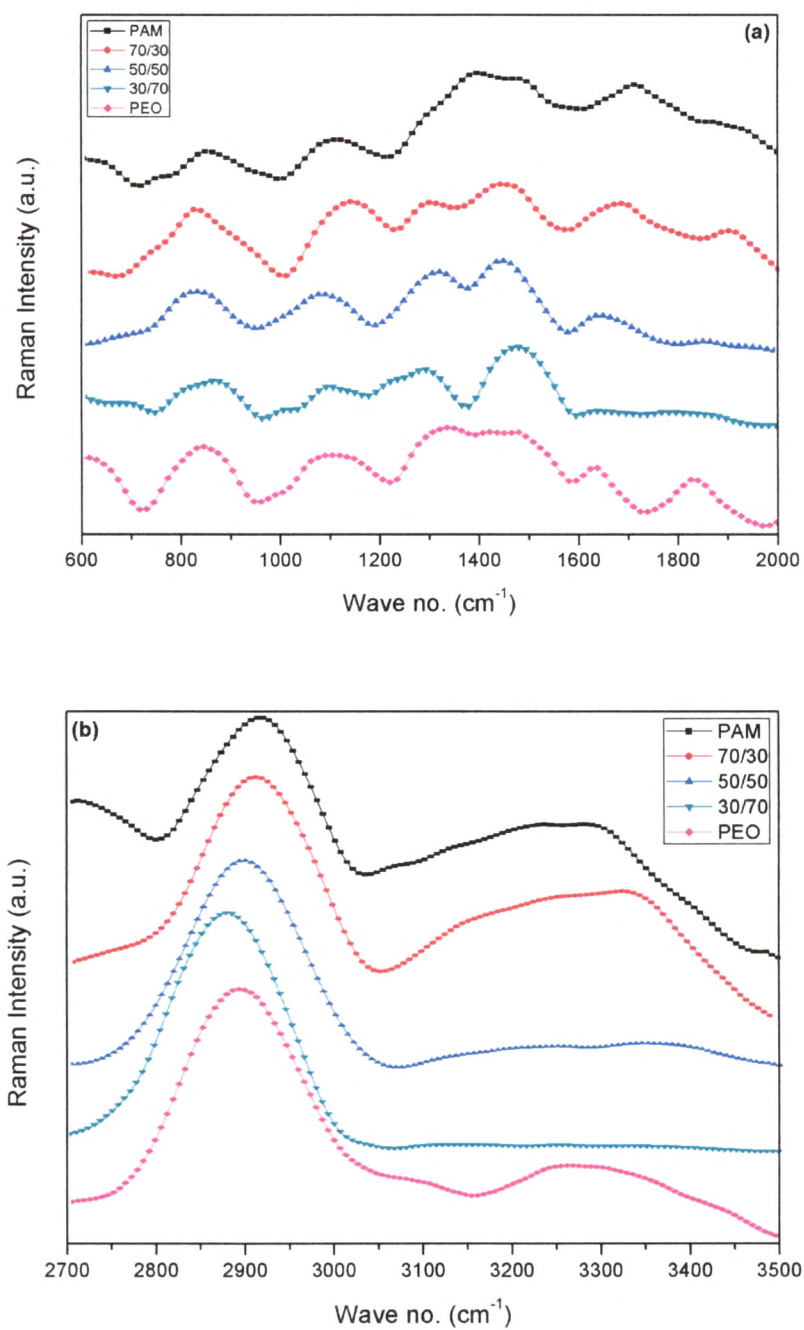


Figure 5.3 Raman spectra of pure and blend films in the range (a) 600-2000 cm⁻¹ (b) 2700-3500 cm⁻¹

Maximum peak shift is observed for 30/70 wt% on lower wave number side which indicates the decrease in bond strength. A simultaneous decrease in the intensities of the lines peaked at 3259 cm^{-1} and 3270 cm^{-1} , which is assigned to the $-\text{NH}_2$ stretching of PAM and $-\text{OH}$ stretching region of PEO respectively. Which is confirmed the interaction between $-\text{CONH}_2$ group of PAM and $-\text{CH}_2\text{OH}$ group of PEO. For these groups, maximum peak shift to higher wave number side is observed for 70/30 wt% (Table 5.3), which indicates the enhancement of bond strength.

We can see that for 30/70 blend ratio, peaks of $-\text{NH}_2$ stretching of $-\text{CONH}_2$ group of PAM and $-\text{OH}$ stretching of $-\text{CH}_2\text{OH}$ group of PEO is almost disappear, which reveals the interaction between these two group of pure polymers. A peak at 1479 cm^{-1} becomes prominent and intense due to interaction, which means $-\text{CONH}_2$ group of PAM convert into $-\text{CH}_2\text{NH}_2$ group due to the interaction with $-\text{CH}_2\text{OH}$ group of PEO [40]. Peaks of $\text{C}=\text{O}$ stretching and $-\text{NH}_2$ stretching are very weak, it also confirm our prediction. From all the Raman spectra, we concluded that hydrogen bonding interaction at molecular level occurs between $-\text{CONH}_2$ group of PAM and $-\text{CH}_2\text{OH}$ group of PEO which confirmed FTIR results.

Table 5.3 Assignments of Raman bands of pure PAM, Pure PEO and PAM/PEO blends [37, 41-42].

PAM	Peak Assignment	PEO	Peak Assignment	70/30 (wt %)	50/50 (wt %)	30/70 (wt %)
854	C-C stretching	847	C-C stretching	833	829	865
1107	C-O-C stretching	1104	C-O stretching	1143	1086	1100
		1336	$-\text{CH}_2$ wagging	1300	1318	1290
1400	C-N stretching	1454	$-\text{CH}_2$ deformation	1460	1450	1479
1711	$\text{C}=\text{O}$ Stretching	1633	$-\text{CH}_2$ twist	1686	1650	weak
2919	$-\text{CH}_2$ stretching	2894	CH_3 stretching	2919	2898	2879
3259	$-\text{NH}_2$ stretching	3270	$-\text{OH}$ stretching	3323	weak	weak

5.2.4. Mechanical Analysis

Mechanical properties of PAM/PEO were taken to study the Max load, Ultimate tensile strength (UTS), young's modulus (Y.M.), stress at break, stiffness and elongation at break for pure and blends films as shown in Figure 5.4. The mechanical properties in blends are changed, because pure polymer matrix provided different cross linking density with different weight% of blended polymer [56]. Those polymers, which have higher crystallinity, cross linking density or rigid chain, they gain a higher strength and lower extensions and therefore polymers with higher young's modulus and ultimate tensile strength value will have lower elongation value [56-58]. When we introduce PEO into PAM polymer matrix, mechanical properties of blends are greatly influenced. From the graph our results also agrees with the above conclusion. For 70/30 blend ratio the YM and UTS values are higher but have lower elongations value. Blend of PEO with PAM successfully improved the mechanical properties. When PEO is blended with PAM,

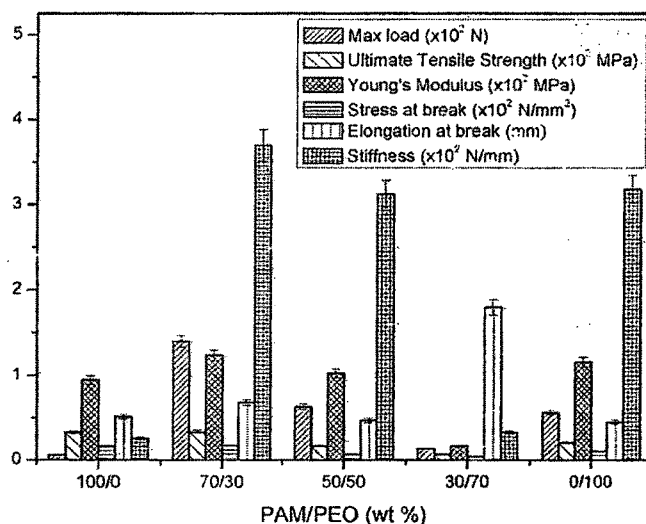


Figure 5.4 Variation in Max load, Ultimate tensile strength, Young's Modulus, stress at break, Elongation at break, Stiffness as a function of PAM/PEO content

interaction at molecular level occurs, which causes the enhancement in mechanical properties. Enhancement in mechanical properties is due to the strong hydrogen bonding between $-\text{CONH}_2$ groups in PAM and $-\text{OH}$ group in PEO. This interaction becomes maximum for 70/30 wt%. Therefore we obtain maximum value of mechanical properties. This can also be correlated with IR analysis. As the maximum higher peak shift was observed for 70/30 wt% which indicates strong bond interaction and hence increase in mechanical properties.

5.2.5. Thermo gravimetric Analysis

Thermogravimetric analysis (TGA) is the most suitable methods for studying the thermal properties of polymers. The TGA and derivative TGA (DrTG) curve provides information about the nature and extent of degradation of the polymers. The effect of blend weight percentage on the TGA and DrTG of PAM/PEO blends are shown in Figure 5.5 (a, b). Detailed information of thermograms is shown in Table 5.4 and Table 5.5.

An important thermal property is the temperature corresponding to the maximum rate of weight loss (T_p), which is defined as the peak value of the first derivative of the TGA curve. T_p was used as a measure of thermal stability. The first derivative curves for pure PAM, pure PEO and their blends are shown in Figure 5.5 (b) and their T_p values are listed in Table 5.4.

Thermal stability of blend is higher than the pure PAM because T_p shifted towards higher temperature. T_p was a maximum for 70/30 wt %, so this blend ratio is more thermally stable. This higher thermal stability was observed for 70/30 wt % blend sample by TGA and DrTG were due to the intermolecular cross linking reaction which gave highly compatible impact blend system [59, 60].

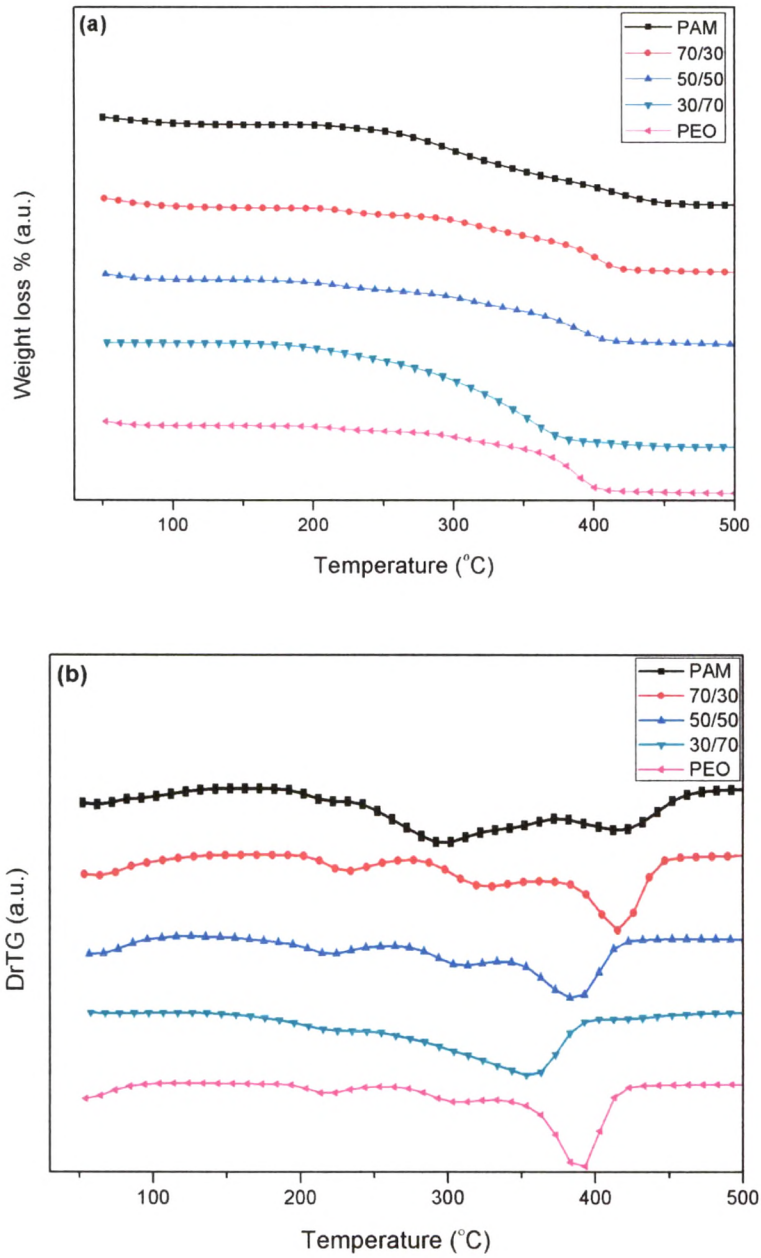


Figure 5.5 (a) TG of pure PAM, pure PEO and blends (b) Dr TG of pure PAM, pure PEO and blends

Table 5.4 TG and DrTG data of Pure PAM, PEO and their blended samples

PAM/PEO	Temperature(°C)		
	Starting	Ending	T _p
100/0	184	220	203
	230	369	294
	377	489	415
70/30	190	254	218
	265	335	308
	350	503	391
50/50	150	253	214
	262	331	302
	341	457	385
30/70	130	238	214
	248	403	357
0/100	183	249	216
	260	328	305
	336	443	383

Table 5.5 Effect of the Blend Ratio on the Temperatures Corresponding to Different Percentage Weight Losses in PAM/PEO Blends

PAM/PEO Blend	T ₃₀ (°C)	T ₄₀ (°C)	T ₅₀ (°C)	R ₅₀₀ (%)
100/0	290	311	334	9.77
70/30	304	330	361	17.75
50/50	300	329	358	15.19
30/70	284	305	321	0.15
0/100	337	363	376	12.50

Table 5.5 gives an idea about the effect of the blend ratio on the temperature corresponding to different weight losses (viz. T_{30} = temperature corresponding to 30 wt % degradation, and so on). It is observed from the table 5 that the 70/30 wt% had maximum temperature value for different weight losses. So we can conclude that the 70/30 wt% have greater thermal stability as compared to pure component. R_{500} indicate the residue value of polymer content at 500 °C. This value was also higher for the blend ratio of 70/30 wt%. From TGA, we conclude that the thermal stability regions of the blended samples were higher than the PAM and stability enhanced by increasing PEO content in PAM polymer matrix and it becomes more stable for 70/30 wt%. The thermal stability regions of the blended samples were higher than the PAM and stability enhanced by increasing PEO content in PAM polymer matrix and it becomes more stable for 70/30 wt%. This indicates the possibility of a strong bonding between PAM and PEO due to $-\text{CONH}_2$ groups in PAM and $-\text{OH}$ group in PEO, which is also confirmed by our FTIR study.

5.2.6. Differential Scanning Calorimeter Analysis

To get the information regarding the different phase transitions temperature, DSC measurements have been carried out on the prepared samples. The DSC plot of the investigated (PAM/PEO) polymer blend is shown in Figure 5.6 (a). The melting temperature T_m of the polymer blends depends on the PEO concentration. The melting temperature (T_m) for pure PEO is observed around 67.65 °C where as it is shifted to 64.88, 67.20 and 72.09 °C in 70/30, 50/50 and 30/70 wt% of PAM/PEO blend films, respectively. DSC provides a quick method for determining polymer crystallinity. PAM does not showed melting peak in the DSC operation range, so heat of fusion values calculated from the melting peaks were considered for PEO portions.

The crystallinity (χ_c) of PEO in blend films was calculated from DSC data according to the following equation $\chi_c = \Delta H / f_w \Delta H_0$ [61]. Where, ΔH_0 is heat of fusion or melting enthalpy for

per gram of 100% crystalline PEO(=213.7 J/g) [62]. f_w is the weight fraction of PEO and ΔH is heat of fusion or melting enthalpy of blend sample. The calculated melting enthalpy and the value of degree of crystallinity χ_c (%) is shown in **Table 5.6**. In the present investigation, the degree of crystallinity of (PAM/PEO blend) polymers increases with concentration of PEO increases. The increment of crystallinity of polymer blends show that the PEO interacts strongly with the PAM.

Table 5.6 T_m (°C), ΔH (J/g), χ_c (%), of PAM/PEO Blends

PAM/PEO blend (wt%)	T_m (°C)	ΔH (J/g)	χ_c (%)
100/0	-	-	-
70/30	64.88	86.58	12.16
50/50	67.20	113.2	26.49
30/70	72.09	89.59	29.35
0/100	67.65	124.2	58.12

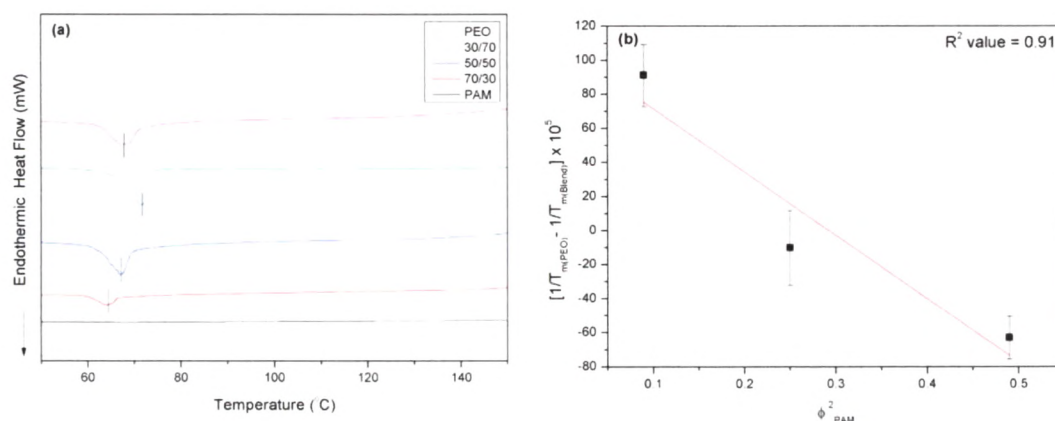


Figure 5.6 (a) DSC curve of pure PAM, pure PEO and blends (b) Dependence of $\frac{1}{T_{m(PEO)}} - \frac{1}{T_{m(Blend)}}$ with ϕ_{PAM}^2 for PAM/PEO blends

From the Flory-Huggins theory, Polymer-polymer interaction parameter can be calculated with the help of below Nishi-Wang equation [63]:

$$\frac{1}{T_{m(PEO)}} - \frac{1}{T_{m(blend)}} = \left[\frac{R V_{PEO}}{V_{PAM} \Delta H_{PEO}} \right] \chi_{12} \phi_{PAM}^2$$

Where V_{PEO} and V_{PAM} is the molar volume of the repeating unit of the polymer; ΔH_{PEO} is the melting enthalpy of fully crystalline PEO; ϕ is the volume fraction; χ_{12} is the polymer-polymer interaction parameter, R is the universal gas constant. From the above parameter for the blends and the evaluation of polymer -polymer interaction and hence miscibility of the system were performed. It can be shown that negatives values for the χ_{12} are correlated to existence of interactions between the polymers, thus resulting in the miscibility of the system.

Figure 5.6(b) shows the curve of $\frac{1}{T_{m(PEO)}} - \frac{1}{T_{m(blend)}}$ vs ϕ_{PAM}^2 . The slope of the line is related to the value of χ_{12} . If the negative slope is obtained then value of χ_{12} is negative which reveals the system is miscible. For PAM/PEO blend the interaction parameter χ_{12} was calculated using below parameter.

$$R = 8.314 \text{ J}\cdot\text{K}^{-1}\cdot\text{mol}^{-1},$$

$$\Delta H_{PEO} = 7.6 \text{ J}\cdot\text{K}^{-1}\cdot\text{mol}^{-1},$$

$$V_{PEO} = 40.3 \times 10^{-6} \text{ m}^3\cdot\text{mol}^{-1},$$

$$V_{PAM} = 24.09 \times 10^{-6} \text{ m}^3\cdot\text{mol}^{-1}$$

The value of χ_{12} is equal to -203.7 so the negative value for χ_{12} indicated miscibility of polymers.

5.2.7. Scanning Electron Microscopy

Figure 5.7 (a-e) shows scanning electron micrographs of the fracture surfaces of PAM and PEO and PAM/PEO blend with different composition. SEM micrographs clearly show the changed surface morphologies of the different blends as compared to pure polymers. As shown in Figure 5.7 (a, e), surface of PAM and PEO are very smooth, showing only a limited number of small particles dispersed along the micrograph. As we increase the fraction of PEO in the PAM polymer matrix, surface appears heterogeneous due to enhanced volume fraction of polymer. From the blend's micrographs, (Figure 5.7 (b-d)), we concluded that as we added PEO in PAM polymer matrix, polymer chains form irregular shaped clusters. But for 70/30 wt% quite homogeneous surface obtained with good dispersion of PEO. This may be attributed to the formation of hydrogen bonding between two polymers [64]. This also confirmed our FTIR results. From Figure 5.7 (c, d) surface appears packed in, separated domains and porous for 50/50 wt % and 30/70 wt %. While from Figure 5.7 (b) surfaces are quite homogeneously dense and much reduced domains with good dispersed PEO particle in PAM polymer matrix, which show the maximum strong intermolecular interaction between PAM and PEO for 70/30wt%, which is also correlated with DSC result. Crystallinity is increases as percentage of PEO increases, so we get rougher surface for 50/50 and 30/70 wt% other than 70/30 wt%. From SEM micrograph 70/30 wt% blend is miscible so hydrogen bond taking place[64]. Hence 70/30 wt% had more thermally stable and have higher mechanical properties. These results also correlated with FTIR conclusion.

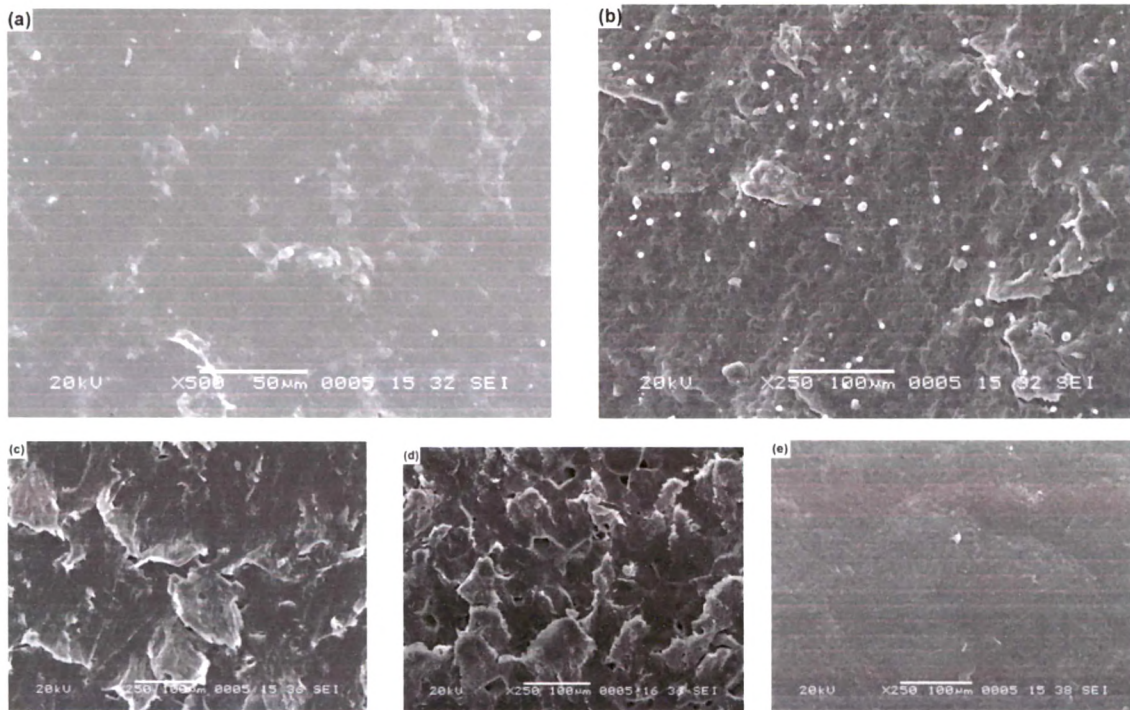


Figure 5.7 Scanning Electron Micrograph of (a) Pure PAM (b) 70/30 (c) 50/50 (d) 30/70 (e) Pure PEO

5.3. Conclusions

FTIR and Raman analysis showed that when PEO blend with PAM, blend components exhibited significant interaction with each other via hydrogen bonding between $-\text{CONH}_2$ groups in PAM and $-\text{CH}_2\text{OH}$ group in PEO. This intermolecular interaction is maximum for 70/30 wt% which exhibited the strong bond interaction and due to this it has maximum thermal and mechanical properties. Optical spectra provide proof for interaction between PAM and PEO. The shift of the absorption edge in the blends reflects the variation in the energy gap which arises due to the intermolecular interaction between PAM and PEO. DSC analysis showed the increment of crystallinity as increases PEO wt% and also the negative value for polymer-polymer interaction parameter χ_{12} indicated miscibility of polymers. SEM micrograph also showed the good dispersion and homogeneity for 70/30 wt% of PAM/PEO blend. Miscibility of the polymer is

also confirmed by SEM micrograph. So from this study we concluded that blend of PAM/PEO with 70/30 wt% is most suitable and compatible with most enhancing properties.

5.4. References

1. Sauchez IC. Bulk and Interface-thermodynamics of polymer alloys. Annual review of material science, 13; 387-412, 1983. [DOI: 10.1146/annurev.ms.13.080183.002131]
2. Utracki LA. Polymer blends handbook. Kluwer Academic Publishers; Vol. 2; ISBN-13: 9781402011146, 2003.
3. Florence Croisier, Christine Jérôme. European Polymer Journal; 49(4); 780–792, 2013. [DOI: <http://dx.doi.org/10.1016/j.eurpolymj.2012.12.009>]
4. Caykara T, Demirci S. Polym Plast Tech & Engg; 2007; 46(7); 737–741, 2007.[DOI:10.1080/03602550701273971]
5. Yuk SH, Cho SH, Lee HB. J Controlled Release; 37; 69–74, 1995. [[http://dx.doi.org/10.1016/0168-3659\(95\)00065-G](http://dx.doi.org/10.1016/0168-3659(95)00065-G)]
6. Araya-Hermosilla R, Broekhuis AA, Picchioni F. European Polymer Journal; 50; 127–134, 2014. [<http://dx.doi.org/10.1016/j.eurpolymj.2013.10.014>]
7. Dean K, Yu L, Bateman S, Dong YW. J Appl Polym Sci; 103(2), 802–811, 2007. [DOI: 10.1002/app.25149]
8. Mruthyunjaya S, Swamy TM. J Macro Sci; 44(3); 321–327. [DOI:10.1080/10601320601077492]
9. Imre B, Pukánszky B. European Polymer Journal; 49; 1215–1233, 2013; [<http://dx.doi.org/10.1016/j.eurpolymj.2013.01.019>]
10. Caulfield MJ, Qiao GG, Solomon DH. Chem Rev; 102(9); 3067-3084, 2002. [DOI: 10.1021/cr010439p]
11. Lopatin VV, Askadskii AA, Peregudov AS, Vasilev VG. J Appl Polym Sci; 96(4); 1043–1058, 2005. [DOI: 10.1002/app.21477]
12. Abdelhak M, Abdelkarim H, Barbara I. J Chem Chem Eng; 6; 7-17, 2012. [ISSN: 1934-7375]
13. Wever DA, Picchioni F, Broekhuis AA. European Polymer Journal; 49; 3289–3301, 2013. [<http://dx.doi.org/10.1016/j.eurpolymj.2013.06.036>]
14. Gavrilin MV. Pharm Chem J; 35(1); 35–39, 2001. [DOI: 10.1023/A:1010402826818]

15. Suzuki H, Miyemoto N, Masad T, Hayakawa E, Ito K. *Chem Pharm Bull (Tokyo)*; 44(2); 364–371, 1996. [DOI: <http://dx.doi.org/10.1248/cpb.44.364>]
16. Abderlrazek EM, Ibrahim HS. *Physica B*; 405; 4339-4343, 2010. [Doi:10.1016/j.physb.2010.07.038]
17. Lee K Y, Yuk SH. *Progress in Polymer Science*; 32(7); 669–697, 2007. [DOI: <http://dx.doi.org/10.1016/j.progpolymsci.2007.04.001>]
18. Parmar AV, Bahadur A, Kuperkar K, Bahadur P. *European Polymer Journal*; 49; 12–21, 2013. [DOI:10.1016/j.eurpolymj.2012.10.009]
19. Salmaso S, Semenzato A, Bersani S, Matricardi P, Rossi F, Caliceti P. *International Journal of Pharmaceutics*; 345; 42–50, 2007. [DOI: <http://dx.doi.org/10.1016/j.ijpharm.2007.05.035>]
20. Pereira AG, Paulino AT, Rubira AF, Muniz EC. *eXPRESS Polymer Letters*; 4(8); 488–499, 2010. [DOI: 10.3144/expresspolymlett.2010.62]
21. Pereira AG, Paulino AT, Nakamura CV, Britta EA, Rubira AF, Muniz EC. *Materials Science and Engineering C*; 31(2); 443–451, 2011. [DOI: <http://dx.doi.org/10.1016/j.msec.2010.11.094>]
22. Sim LH, Gan SN, Chan CH, Kammer HW, Yahya R. *Materials Research Innovations*; 13(3); 278–281, 2009. [DOI: 10.1179%2F143307509X440523]
23. Kiran Kumar K, Ravi M, Pavani Y, Bhavani S, Sharma AK, Narasimha Rao VV. *Physica B*; 406; 1706–1712, 2011. [doi:10.1016/j.physb.2011.02.010.]
24. Reddeppa N, Sharma AK, Narsimha Rao VV, Chen W. *Microelectronic Engineering*; 112; 57–62, 2013. [<http://dx.doi.org/10.1016/j.mee.2013.05.015>]
25. Elashmawi IS, Abdelrazek EM, Hezma AM, Rajeh A. *Physica B*; 434; 57–6, 2014.. [<http://dx.doi.org/10.1016/j.physb.2013.10.038>.]
26. Ferreira V, Douglas JF, Warren J, Karim A. *Phys Rev E*; 65; 042802-[1-4], 2002. [DOI: 10.1103/PhysRevE.65.042802]
27. Ferreira V, Douglas JF, Warren J, Karim A. *Phys Rev E*; 65; 051606-[1-16], 2002. [DOI: 10.1103/PhysRevE.65.051606]

28. Sawatari Ch, Kondo T. *Macromolecules*; 32; 1949-1955, 1999. [DOI: 10.1021/ma980900o]
29. Zheng H, Zheng S, Guo Q. *J Polym Sci A Polym Chem*; 35; 3169–3179, 1997. [DOI: 10.1002/(SICI)1099-0518(19971115)35:15<3169::AID-POLA10>3.0.CO;2-9]
30. Vijayalakshmi SP, Madras G. *J Appl Polym Sci*; 101; 233–240, 2006. [DOI 10.1002/app.23246.]
31. Vijayalakshmi SP, Raichar A, Madras G. *J Appl Poly Scie*; 101; 3067–3072, 2006. [DOI 10.1002/app.24115]
32. Pielichowska K, Głowinkowski S, Lekki J, Binias D, Pielichowski K, Jenczy J. *European Polymer Journal*; 44(10); 3344–3360, 2008. [DOI: <http://dx.doi.org/10.1016/j.eurpolymj.2008.07.047>]
33. Sowwan M, Faroun M, Musa I, Ibrahim I, Makharza S, Sultan W, Dweik H. *Int J Phy Sci*; 3(6); 144–147, 2008. [ISSN 1992–1950]
34. Colthup NB, Daly LH, Berley SE. *Introduction to Infrared and Raman Spectroscopy* (3rd edition); Academic press INC. Elsevier; 1990. [ISBN 0080917402, 9780080917405]
35. Chen N, Zhang J. *Chinese Journal of Polymer Science*; 28(6); 903-911, 2010. [DOI: 10.1007/s10118-010-9167-x]
36. Gaurang Patel, Mundan B Sureshkumar. *Iran Polym J*; 2013. [DOI: 10.1007/S 13726-013-0211-x.]
37. Guo C, Liu H, Wang J, Chen J. *Journal of Colloid and Interface Science*; 209; 368-373, 1999. [DOI: Jcis.1998.5897]
38. Bostan MS, Mutlu EC, Kazak H, Keskin SS, Oner ET, Eroglu MS. *Carbohydrate polymers*; 2013. [DOI: <http://dx.doi.org/10.1016/j.carbpol.2013.09.096>]
39. Dong J, Fredericks PM, George GA. *Polym Degrad Stab*; 58; 159-169, 1997. [DOI: [http://dx.doi.org/10.1016/S0141-3910\(97\)00040-2](http://dx.doi.org/10.1016/S0141-3910(97)00040-2)]
40. Lee JH, Jung HW, Kang IK, Lee HB. *Biomaterials*; 15(9); 705-711, 1994. [[http://dx.doi.org/10.1016/0142-9612\(94\)90169-4](http://dx.doi.org/10.1016/0142-9612(94)90169-4)]

41. Sundaraganesan N, Puviarasan N, Mohan S. *Talanta*; 54; 233-241, 2001. [http://dx.doi.org/10.1016/S0039-9140(00)00585-3]
42. A da costa AM, Amada AM. *Polymer*; 41(4); 5361-5365, 2000. [DOI: http://dx.doi.org/10.1016/S0032-3861(99)00732-6]
43. John RD. *Applications of Absorption Spectroscopy of Organic Compounds*. Prentice-Hall Inc.; 1965. [ISBN: 0130388025]
44. Srivastava AK, Virk HS. *Journal of Polymer Materials (Netherlands)*, 17(3), 325-328, 2000.
45. Rajesh Kumar, Asad Ali S, Mahur AK, Virk HS, Singh F, Khan SA, Avasthi DK, Rajendra Prasad. *Nucl Instr and Meth in Phys Res B*; 266(8); 1788-1792, 2008. [http://dx.doi.org/10.1016/j.nimb.2008.01.010]
46. Gaurang Patel, MB Sureshkumar, Purvi Patel. *AIP Conf Proc*; 1349; 166-167, 2011. [DOI: 10.1063/1.3605788]
47. Tauc J, Grigorovici R, Vanku A. *Phys Stat Sol (b)*; 15(2); 627-637, 1996. [DOI: 10.1002/pssb.19660150224]
48. Shahada L, Kassem ME, Abdelkader HI, Hassan HM. *J Appl Polym Sci*; 65(9); 1653-1657, 1997. [DOI: 10.1002/(SICI)1097-4628(19970829)65:9<1653::AID-APP1>3.0.CO;2-E].
49. Mott NF, Davis EA. *Electronic processes in Non Crystalline materials*. 2nd edition; Oxford university press; USA; 1979. [ISBN: 0198512880]
50. S Kilarkaje, Manjunatha V, Raghu S, Ambika Prasad MV, Devendrappa H. *J. Phys. D: Appl. Phys.*, 44, 105403, 2011. [DOI: doi:10.1088/0022-3727/44/10/105403]
51. Nouh SA, *Radiation Measurement*; 38(2); 167-172, 2004. [DOI: http://dx.doi.org/10.1016/j.radmeas.2003.11.004]
52. Singh NL, Sharma A, Avasthi DK. *Nucl Instrum Methods B*; 206; 1120-1123, 2003. [DOI: http://dx.doi.org/10.1016/S0168-583X(03)00935-2]
53. Buttafava A, Consolati G, Di Landro L, Mariani M. *Polymer*; 43(26); 7477-7481, 2002. [DOI: http://dx.doi.org/10.1016/S0032-3861(02)00708-5]

54. Mishra R, Tripathy SP, Sinha D, Dwivedi KK, Ghosh S, Khathing DT, Muller M, Fink D, Chung WH. Nucl Instrum Methods B; 168(1); 59-64, 2000. [DOI: [http://dx.doi.org/10.1016/S0168-583X\(99\)00829-0](http://dx.doi.org/10.1016/S0168-583X(99)00829-0)]
55. Lakshmi GB VS, Ali V, Siddiqui A M, Kulriyac PK, Zulfequar M. Radiat Eff Defects in Solid; 164(3); 162-169, 2009. [DOI: 10.1080/10420150902764186]
56. Patel G, Sureshkumar MB, Singh NL, Bhattacharya SS. Journal of International Academy of Physical Sciences. 14; 91-100, 2010. [ISSN 0974 - 9373]
57. Chi SK, Seung MO.. Electrochim acta; 46; 1323-1331, 2001. [DOI: [http://dx.doi.org/10.1016/S0013-4686\(00\)00727-1](http://dx.doi.org/10.1016/S0013-4686(00)00727-1)]
58. Gaurang Patel, M B Sureshkumar, Purvi Patel. AIP Conf Proc; 1391; 645-648, 2011. [DOI: 10.1063/1.3643636]
59. El-Kader FH, Gafer SA, Basha AF, Bannan SI, Basha MAF. J Appl Polym Sci; 118(1); 413-420, 2010. [DOI: 10.1002/app.30841]
60. Aggour YA. Polm. Degrade. Stab; 51(3); 265-269, 1996. [DOI: [http://dx.doi.org/10.1016/0141-3910\(95\)00205-7](http://dx.doi.org/10.1016/0141-3910(95)00205-7)]
61. Jurkin, T., & Pucic, I. Radiation Physics and Chemistry, 81, 1303-1308, 2012.
62. Shin JH, KimKW, Ahn HJ, Ahn JH, JMater Sci Eng, B 95:148, 2002.
63. A. G. B. Pereira, A. T. Paulino, A. F. Rubira, E. C. Muniz, eXPRESS Polymer Letters Vol.4, No.8, 488-499, 2010.
64. Shefali Mishra, Bajpai R, Katare R, Bajpai AK. J Mater Sci: Mater Med; 17(12); 1305-1313, 2006. [DOI: 10.1007/s10856-006-0605-9]